Graefe's Archive for Clinical and Experimental Ophthalmology
https://doi.org/10.1007/s00417-020-04671-2

GLAUCOMA

Structural imaging of conjunctival filtering blebs in XEN gel implantation and trabeculectomy: a confocal and anterior segment optical coherence tomography study

Matteo Sacchi[1] · Luca Agnifili[2] · Lorenza Brescia[3] · Francesco Oddone[3] · Edoardo Villani[1] · Paolo Nucci[1] · Leonardo Mastropasqua[2]

Received: 4 December 2019 / Revised: 26 March 2020 / Accepted: 30 March 2020

Abstract

Purpose To describe and compare the conjunctival filtering bleb features after XEN gel implantation and trabeculectomy using anterior segment optical coherence tomography (AS-OCT) and in vivo confocal microscopy (IVCM).

Methods Fifty-two patients who underwent completely successful trabeculectomy (24 eyes) or completely successful XEN gel implantation (28 eyes) were consecutively enrolled. At the sixth-month follow-up, filtering blebs were analyzed with AS-OCT and IVCM. The main outcomes were the following: (i) bleb-wall epithelium cyst-like structure density and area (BECSD, BSCSA), (ii) bleb-wall sub-epithelium cyst-like structure density and area (BSCSD, BSCSA,), (iii) bleb-wall thickness (BT), (iv) bleb-wall epithelial thickness (BET), (v) bleb-wall reflectivity (BR), and (vi) bleb height (BH), for AS-OCT. Mean microcyst density (MMD) and area (MMA) and stromal meshwork reflectivity (SMR) were the IVCM outcomes.

Results Six-month intraocular pressure was 11.46 ± 3.09 and 10.06 ± 3.39 mmHg in the XEN gel implantation and trabeculectomy, respectively ($p > 0.05$). At AS-OCT, XEN gel blebs showed lower BH, BT, BET, BR, ($p < 0.001$), and BECSA values ($p < 0.005$), and a higher BECSD ($p < 0.05$) compared with trabeculectomy blebs. At IVCM, MMA and SMR values were lower in the XEN gel implantation, compared with trabeculectomy ($p < 0.05$). BECSD and BSCSD negatively correlated with BR ($p < 0.01$; $r = -0.110$; $p < 0.01$; $r = -0.249$), whereas BR strongly correlated with SMR ($p < 0.001$; $r = 0.819$).

Conclusion Successful filtering blebs after XEN gel implantation appeared flatter and thinner, with a higher number of epithelial cysts and a hypo-reflective bleb wall compared with trabeculectomy. These aspects may depend on the different intra-operative tissue manipulation and/or on different aqueous humor dynamics in the sub-conjunctiva between surgeries.

Keywords Glaucoma · XEN gel implantation · Trabeculectomy · Filtration blebs · In vivo confocal microscopy · Anterior segment optical coherence tomography

Introduction

Trabeculectomy is still considered the gold standard and most performed surgical procedure in the glaucoma treatment algorithm, after medical and laser approach failed [1]. Nevertheless, although effective, trabeculectomy is an operator-dependent technique counting several surgical steps crucial to the final outcome, including scleral flap dissection and suture, scleral ostium creation, MMC application, and conjunctival suturing. Moreover, trabeculectomy may be associated with serious and potentially vision-threatening complications including choroidal effusion, endophthalmitis, hypotony, and visual loss [2].

In order to improve the predictability and the safety profile of the glaucoma surgery, less invasive surgical approaches have been developed in the last years and are nowadays available for clinical practice [3].

The XEN gel implant (Allergan, Dublin, Ireland) is a 6-mm, biocompatible gelatin device with a 45-μm lumen

✉ Luca Agnifili
l.agnifili@unich.it

[1] University Eye Clinic, San Giuseppe Hospital, University of Milan, Milan, Italy

[2] Ophthalmology Clinic, Department of Medicine and Aging Sciences, University G. d'Annunzio of Chieti-Pescara, Via dei Vestini, 66100 Chieti, CH, Italy

[3] IRCCS Fondazione G.B. Bietti, Rome, Italy

Published online: 15 May 2020

forming a conjunctival filtration bleb after ab interno implantation. Because of the ab interno approach, the main advantage of the XEN gel implantation (XGI) is the minimal tissue manipulation, with Tenon's and conjunctival sparing [4]. The XGI shares with the conventional trabeculectomy the formation of a filtering bleb, which allows the procedure to be considered a real filtration surgery. In a multicenter retrospective study comparing XGI with trabeculectomy, the two techniques showed a similar efficacy with a good safety profile of the XGI [4].

The bleb morphology evaluation represents a crucial step during the post-operative follow-up, with a non-inflamed and avascular appearance of the bleb wall, and the presence of numerous microcysts within the epithelium being considered clinical indicators of a good filtration ability [5, 6]. Different clinical grading scales have been proposed to evaluate the filtration ability; however, these scales are subjective and cannot provide microstructural information [5, 7, 8].

In the last decade, the use of diagnostic tools such as laser scanning in vivo confocal microscopy (IVCM) [9–14] and anterior segment optical coherence tomography (AS-OCT) [13, 15–18] greatly improved the filtration bleb assessment, providing objective information at a cellular level [19–21]. These techniques have been recently also used to evaluate the conjunctival bleb features after XEN gel implantation [22–25]. However, to date, no previous studies compared the morphology of the XEN bleb with that of trabeculectomy by using IVCM and AS-OCT. The aim of the present work was to analyze and compare the conjunctival filtration bleb morphology after completely successful XGI and trabeculectomy by using both IVCM and AS-OCT, in order to define macro- and microstructural differences induced by these surgical procedures.

Methods

This was a cross-sectional, observational, double-center, comparative study that consecutively enrolled open angle glaucoma patients who underwent XGI or trabeculectomy between January 1, 2016, and September 30, 2018. The study was carried out at the Ophthalmic Clinic, San Giuseppe Hospital, University of Milan, and the Ophthalmic Clinic, University G. d'Annunzio of Chieti-Pescara, Italy. The study and data accumulation were carried out with the approval from the local institutional review boards and adhered to the tenets of the Declaration of Helsinki.

We retrospectively analyzed electronic medical records as well as IVCM and AS-OCT images of filtering blebs of 52 consecutive glaucomatous patients who underwent successful XGI (28 patients, 28 eyes; XEN gel implantation group) or trabeculectomy (24 patients, 24 eyes; trabeculectomy group). The six-month follow-up data were considered for the analysis.

Patients had to respect the following inclusion criteria: (A) before surgery: (i) open angle glaucoma (primary open angle, pseudo-exfoliative, pigmentary, or normal tension glaucoma), (ii) unmet target intraocular pressure (IOP) despite maximum tolerated medical therapy (including also oral acetazolamide), (iii) a significant progression of the optic nerve damage confirmed on three consecutive reliable visual fields (VF) ((Humphrey field analyzer II 750 (Carl Zeiss Meditec Inc., Dublin, CA) (30-2 test, full-threshold)); (B) after surgery: completely successful XGI or trabeculectomy, which was defined as a third reduction of the baseline IOP without the adjunct of IOP-lowering medications. Eyes that underwent combined cataract and glaucoma surgery were also considered eligible.

The exclusion criteria were anterior chamber intraocular lens, previous glaucoma filtration surgery or retinal or corneal graft surgery, neovascular or uveitic glaucoma, iridocorneal endothelial syndrome, and Axenfeld-Rieger syndrome; in order to avoid biases on the natural features of the filtration blebs, patients who experienced intra- or post-operative complications or were on qualified success were also excluded from the analysis.

A review of the medical charts was conducted and the following demographic and clinical data were collected: age, gender, ethnicity, diabetes status, best-corrected visual acuity (BCVA), baseline IOP, number and type of glaucoma medications, glaucoma diagnosis, VF mean deviation, and history of previous cataract surgery.

For the purpose of this study, we collected and analyzed the IVCM and AS-OCT images of functional conjunctival bleb acquired at the sixth-month follow-up after completely successful surgery. Images were analyzed by the same expert investigator (LA) who was blind for the surgical technique and patient history; moreover, in order to maintain the investigator blind, AS-OCT images where scleral flap or the XEN implant were visible were not included in the analysis.

AS-OCT analysis

The RTVue XR Avanti (RTVue, Optovue, Inc., Fremont, CA, USA) was used for the filtration bleb assessment. By using the anterior segment cornea module lens, the "auto" mode and the CL-line scan 6 mm length, five images for each eye were acquired by a single qualified AS-OCT operator for each center (MS, Milan; LB, Chieti). The details of the AS-OCT examination were previously described [13, 15]. Conjunctival filtration bleb images were acquired with the eye in downward gaze, between the two red-guided lines. Images were analyzed by a second qualified operator, which was masked for the grouping and patient surgical history (EV).

The following AS-OCT parameters were considered, using the ImageJ software (https://imagej.nih.gov/ij/): (i) bleb-wall epithelium cyst-like structure density and area (BECSD and BSCSA, respectively): hypo-reflective round- or oval-shaped cystic structures located within the conjunctival epithelium; (ii) bleb-wall sub-epithelium cyst-like structure density and area (BSCSD and BSCSA, respectively): hypo-reflective round- or oval-shaped cystic structures located between the basal membrane of the bleb-wall epithelium and the scleral surface; (iii) bleb-wall thickness (BT), calculated at the maximum elevation point of the filtration bleb, between the outer and inner limit of the bleb wall; (iv) bleb-wall epithelial thickness (BET), calculated between the conjunctival epithelial surface and the basal membrane of the epithelium; (v) bleb-wall reflectivity (BR), calculated by using ImageJ, and defined as the mean gray value obtained in three non-contiguous points of the bleb wall; and (vi) bleb height (BH) , calculated at the maximum elevation point of the bleb, from the scleral bed to the epithelial surface. Figure 1 shows the bleb-related AS-OCT parameters.

IVCM technique and images analysis

In order to avoid biases due to the mechanical compression, IVCM of filtration bleb was performed just after the AS-OCT evaluation. The digital confocal laser scanning microscope (HRT III Cornea Module, Heidelberg Engineering GmbH, Germany) was used to investigate the epithelial and stromal bleb-wall features. The epithelial analysis aimed at identifying particular extracellular structures named as microcysts; the stromal analysis aimed at analyzing the tissue reflectivity. The technical characteristics of the instrument and the details of the examination were previously described [9–14].

The following parameters were considered: (i) mean microcysts density (MMD; cysts/mm^2); (ii) mean microcyst area (MMA; mm^2); and (iii) stromal meshwork reflectivity (SMR). Images were acquired at the epithelial and sub-epithelial layers (up to 50 μm of depth) of the bleb wall to analyze microcysts, and deeper (up to 150 μm of depth) to evaluate the stromal reflectivity. Bleb-wall microcysts correspond to round- or oval-shaped and differently sized extracellular optically clear structures, described in functional filtering blebs as indicators of efficient aqueous humor drainage [9–14, 26]. SMR represents an indirect indicator of the collagen content within the conjunctival stroma and was graded as previously described (grade 0: normal reflectivity, with thin collagen fibers presenting a regular and straight course; grade 1: mild reflectivity, with thin collagen fibers less regularly organized compared with grade 0, and presenting different orientations; grade 2: moderate regularity, with collagen fibers appearing much thicker and with a less regular course compared with grades 0 and 1; grade 3: high reflectivity, with very thick and disorganized fibers, somewhere presenting as a dense and irregularly homogeneous tissue) [27].

Forty sequential images (400 × 400 mm) derived from automatic scans and manual frames were acquired during each IVCM session, and ten randomly selected high-quality images without artifacts (motion blur and compression lines) were selected for the analysis. A single experienced operator performed IVCM examinations and selected the images for each center (EV, Milan; LA, Chieti); a second operator evaluated the images (FO). Both the operators were masked for the patient surgical history.

The density and area of epithelial microcysts were manually calculated by using the ImageJ software. To define the SMR, a previously used arbitrary grading scale was adopted [27, 28]. SMR was calculated using the ImageJ software by determining the average gray value of images, with the automatic brightness mode selected during examination. This value corresponded to the sum of gray values of all pixels in the entire image divided by the number of pixels. An average gray value less than 90.00 indicated a normal reflectivity (grade 0), from 90.01 to 105.00 mild reflectivity (grade 1), 105.01 to 125.00 moderate (grade 2), and greater than 125.01 high reflectivity (grade 3). Therefore, grades 0 to 3 corresponded to a loosely, mildly, dense, and very dense arranged stromal network, respectively.

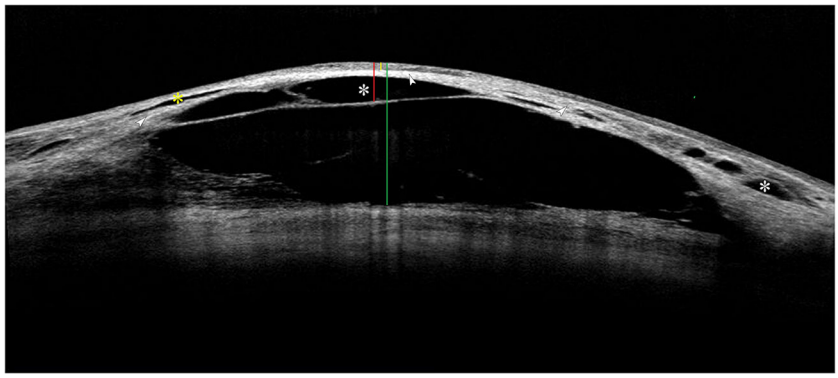

Fig. 1 Representative image reporting the considered AS-OCT parameters. Yellow and white asterisks indicate BECS and BSCS, respectively. Yellow, red, and green lines correspond to BET, BT, and BH, respectively. Arrowheads indicate the areas where BR, expressed in mean gray value, was calculated

Surgical procedures

XEN gel implantation technique

XGI surgeries were performed under topical anesthesia. The XGI was placed in the superior nasal quadrant after 0.1 ml of mitomycin-C (MMC) 0.2 mg/ml has been injected within the upper bulbar conjunctiva. The goal of the surgeon was to obtain the XEN gel implant to be positioned following the "3:2:1 rule": 3 mm under the conjunctiva, 2 mm intra-sclerally, and 1 mm left in the anterior chamber. At the end of the surgery, the proper placement of the XEN under the conjunctiva (or Tenon's capsule) and in anterior chamber was verified.

Trabeculectomy technique

All the procedures were performed under peribulbar anesthesia and were augmented with MMC (sponges soaked in 0.2 mg/ml MMC left for 2–3 min under the tenon-conjunctival layer). The conjunctival flap was fornix-based; a punch was used to create a sclerostomy. A 10-0 nylon suture was used for the scleral flap and a 8/0 polyglactin suture for the conjunctiva and tenon.

Post-operative therapy was similar in both groups: as per protocol, topical unpreserved steroids (dexamethasone 0.15%) were tapered in 12 weeks (beginning from five times), whereas topical unpreserved antibiotics were prescribed for 2 weeks (levofloxacin 5 mg/ml four times daily).

Bleb manipulation procedures were performed when needed, according to the type of surgery.

Statistical analysis

Analysis was performed by SPSS Advanced Statistical TM 20.0 Software (2011; Chicago, IL, USA). The normal distribution of data was tested using the Shapiro-Wilk test. Independent samples *t* test was used to evaluate age, IOP, visual field mean defect (MD), and gender differences between groups; paired *t* test was used to investigate statistical differences in IOP and MD after surgical procedures, whereas χ^2 test was used to analyze the percentage of phacoemulsification-combined and post-surgical needling procedures between groups. Non-parametric Mann-Whitney *U* test was performed to investigate AS-OCT and IVCM data differences between groups. Correlations among the variables were determined using a non-parametric measure by the Spearman's index. A $p < 0.05$ was considered statistically significant.

Results

The baseline demographic and clinical data of patients are shown in Table 1; no significant baseline differences were found between groups, except for the visual field MD, which was higher in the trabeculectomy group ($p < 0.05$). Thirty-seven percent and 29% of patients in the trabeculectomy and XGI groups, respectively, underwent a combined procedure. Post-surgical 5-fluorouracil augmented procedures were performed in 21% and 14% of patients who underwent trabeculectomy and XGI, respectively, based on an IOP increase over 21 mmHg during post-operative controls [29]. The mean number of post-operative procedures was 1.61 ± 0.34 and 1.41 ± 0.28, in the trabeculectomy and XGI group, respectively; the timing of post-operative procedures was 27.2 ± 13.3 days and 24.5 ± 10.3 days in the trabeculectomy and in the XGI group, respectively.

At the sixth-month follow-up, IOP values did not differ between the two surgical procedures. None of the patients experienced significant intra- or post-operative complications.

AS-OCT

The six-month AS-OCT data are reported in Table 2. Patients who underwent trabeculectomy showed a greater BH compared with the XGI group ($p = 0.001$). Patients who underwent XGI showed a higher BECSD compared with patients who underwent trabeculectomy, whereas BECSA was higher in the trabeculectomy group ($p = 0.034$ and $p = 0.002$, respectively). The sub-epithelial features did not differ between groups, with both BSCSD and BSCSA values similar between the trabeculectomy and the XGI groups. The BT and BET parameters were significantly higher in the trabeculectomy compared with the XGI group ($p = 0.001$ and $p = 0.003$, respectively). The BR was significantly lower in the XGI compared with the trabeculectomy group ($p < 0.001$) (Fig. 2g, h).

IVCM

The six-month IVCM data are reported in Table 3. For the epithelial parameters, MMD was not significantly different between groups, whereas MMA is higher in the trabeculectomy compared with the XGI group ($p = 0.021$) (Fig. 2c, d). The XEN gel bleb group showed significantly lower SMR values compared with the trabeculectomy blebs ($p = 0.011$) (Fig. 2e, f).

Correlations

BSCSD positively correlated with BSCSA and BECSD ($p < 0.01$; $r = 0.183$; $p < 0.01$; $r = 0.098$) and negatively correlated with BET ($p < 0.01$; $r = -0.470$) and BR ($p < 0.01$; $r = -0.249$). BSCSA correlated positively with BR ($p < 0.01$; $r = 0.330$), whereas negatively with BT ($p < 0.01$; $r = -0.213$) and BET ($p < 0.01$; $r = -0.235$). BECSD positively correlated with BET ($p < 0.01$; $r = 0.216$) and negatively with BR

Table 1 Demographic and clinical data of groups

	Age (years)	M/F	Baseline IOP	Sixth-month IOP	Baseline MD	Sixth-month MD	Duration of disease (Mo ± SD)	Combined procedures (%)	Post-surgical needling procedures (%)
XGI	64.73 ± 13.21	12/16	24.84 ± 2.21	11.46 ± 3.09*	− 10.51 ± 8.72§	− 10,53 ± 8.49§	58.76 ± 4.42	29%	14%
Trabeculectomy	69.81 ± 9.95	10/14	25.83 ± 2.98	10.66 ± 3.39*	− 15.20 ± 9.08	− 14.95 ± 8.64	61.32 ± 5.78	37%	21%

*$p < 0.001$ vs baseline IOP (paired *t* test)

§ $P < 0.05$ vs trabeculectomy

Y, years (mean ± SD); *Mo*, months (mean ± SD); *M*, males; *F*, females; *IOP*, intraocular pressure (mmHg; mean ± SD); *MD*, mean defect (dB; mean ± SD)

($p < 0.01$; $r = -0.110$). BECSA positively correlated with BT ($p < 0.01$; $r = 0.240$). BT positively correlated with BET ($p < 0.01$; $r = 0.707$) and BR ($p < 0.01$; $r = 0.097$). Positive correlations were found between BECSD and BECSA with MMD ($p < 0.05$; $r = 0.673$; and $p < 0.01$; $r = 0.552$), and between BR and SMR ($p < 0.001$; $r = 0.819$).

Discussion

The role of imaging tools is becoming increasingly important in the post-operative management of a patient with glaucoma, as they allow an ultrastructural analysis of clinically undetectable structures of the filtering bleb [27, 28].

In the present study, AS-OCT and IVCM revealed significant macroscopic and microscopic differences in the bleb morphology between trabeculectomy and XGI group.

In more detail, IVCM showed a larger microcyst area in the trabeculectomy compared with the XGI group. Several studies observed that functioning blebs after trabeculectomy showed numerous intraepithelial microcysts with a loosely arranged connective stromal tissue in contrast to failed filtering blebs [9–14, 27, 28].

The only study that used IVCM to describe the filtration bleb after XGI reported an MMA increase 12 months after surgery, even though MMA was not significantly different in successful compared with failed blebs [23]. This probably depended, at least in part, on the small sample size of this study.

In our work, successful XGI and trabeculectomy presented a high number of epithelial microcysts within the bleb wall. The greater MMA found in the trabeculectomy group could be explained by the larger scleral ostium obtained with the trabeculectomy compared with the 45-μm lumen of the XEN gel implant, leading to a greater aqueous outflow towards the sub-conjunctival space. This hypothesis seems supported also by the larger BECSA seen with AS-OCT.

On the other hand, we observed an overall bleb-wall reflectivity significantly lower in the XGI compared with trabeculectomy, both with IVCM (stroma) and AS-OCT (entire bleb wall).

As widely reported, with respect to failed blebs, the subepithelial connective tissue of functioning blebs is loosely arranged, hypo-reflective, and contains optically clear spaces [9–11]. These studies considered the hyper-reflective pattern as a sign of collagen deposition and scarring.

In line with IVCM studies on trabeculectomy, Fea and colleagues [23] observed a lower stromal density in successful compared with the unsuccessful XGI [9–11, 13]. Overall, our IVCM and AS-OCT findings were in line with this study since

Table 2 AS-OCT parameters of XGI and trabeculectomy groups

	BSCSD (*n* ± SD)	BSCSA (mm^2 ± SD)	BECSD (*n* ± SD)	BECSA (mm^2 ± SD)	BH (μm ± SD)	BT (μm ± SD)	BET (μm)	BR
XGI	0.85 ± 0.37	3468.04 ± 1308.26	3.23 ± 2.8	206.99 ± 177.95	822.82 ± 138.06	258.43 ± 197.05	37.30 ± 15.24	46.39 ± 15.76
Trabeculectomy	0.58 ± 0.51	4041.64 ± 2235.97	2.92 ± 1.68	293.29 ± 153.71	928.91 ± 109.42	468.71 ± 145.38	48.98 ± 14.13	112.19 ± 29.95
Mann-Whitney *U* test (*p* value)	0.499	0.195	0.034	0.002	0.001	0.001	0.003	< 0.001

XGI, XEN gel implantation; *BSCSD*, bleb-wall sub-epithelium cyst-like structure density; *BECSD*, bleb-wall epithelium cyst-like structure density; *BSCSA*, bleb-wall sub-epithelium cyst-like structure area; *BECSA*, bleb-wall epithelium cyst-like structure area; *BH*, bleb height; *BT*, bleb-wall thickness; *BET*, bleb-wall epithelial thickness; *BR*, bleb-wall reflectivity

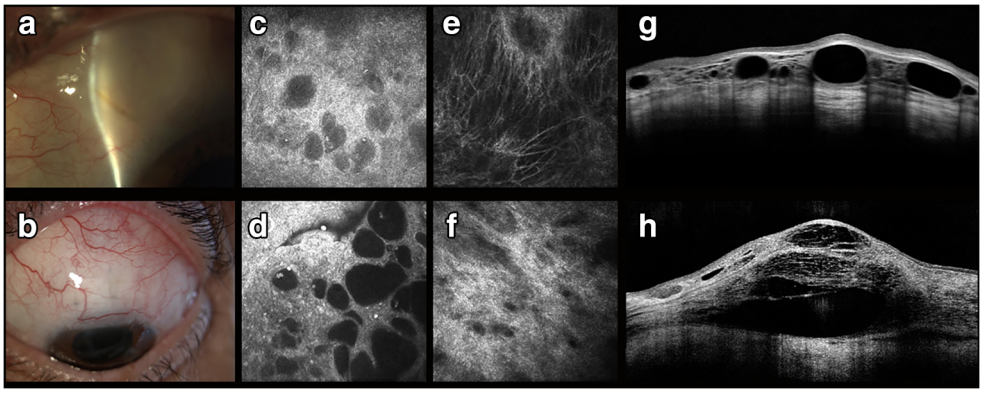

Fig. 2 Slit lamp, IVCM, and AS-OCT images of the XEN gel implant (top line) and trabeculectomy blebs (bottom line). **a**, **b** Slit lamp appearance of successful filtering blebs 6 months after XEN gel implantation (**a**) and trabeculectomy (**b**). **c**–**f** Confocal scans showing conjunctival epithelial microcysts (**c**, **d**) and stromal meshwork reflectivity (**e**, **f**). **g**, **h** AS-OCT images showing bleb-wall epithelium and sub-epithelium cyst-like structures, and differences in the bleb stromal reflectivity between XEN gel implant and trabeculectomy

we observed a lower tissue reflectivity in the XGI compared with trabeculectomy.

During the past decade, several AS-OCT parameters have been proposed to characterize the filtering bleb function after trabeculectomy, and among them, the bleb-wall reflectivity, which is a surrogate sign of fibrosis, presented the strongest correlation with the surgical outcome [13, 16, 17, 19, 20, 30, 31].

Some studies reported that also the bleb-wall thickness significantly correlated with the bleb filtration ability [15, 17, 21, 31].

These data suggest that after trabeculectomy, blebs showing a low degree of reflectivity and a thick wall are more likely to have a good filtering function.

To date, only a few AS-OCT studies investigated the bleb morphology after XGI [22–25]. Fea et al. [23] and Perez et al. [22] confirmed that patients with a low bleb-wall reflectivity were more likely to have a good surgical outcome. Lenzhofer and colleagues [24] found that blebs showing signs of subconjunctival separation with small, diffuse, and hyporeflective cysts were more likely to have lower IOP. Conversely, blebs with a uniform pattern and without fluid-filled hypo-reflective structures were associated to a higher risk of failure. The only study that compared filtration blebs after XGI and the trabeculectomy did not observe conjunctival fibrosis in the XEN group [25]. Our results are in line with this study since we observed a lower BR and SMR after XGI compared with trabeculectomy, with a high correlation between these parameters. These results indicate that functioning XGI blebs present a more loosely arranged connective tissue compared with trabeculectomy. This aspect could depend by the fact that conjunctiva and Tenon's capsule are almost completely spared during XGI; in addition, in the XGI, MMC is injected and left under the conjunctiva, whereas in trabeculectomy, MMC is sponged and washed out after its application.

In this work, we introduced four new AS-OCT parameters, BECS and BSCS density and area, inspired by the study of Narita and colleagues [31] that described small hyporeflective spaces within or beneath the epithelial layer of functioning blebs, and by the study of Nakano et al. [16], which found that blebs with microcystic and sub-conjunctival separation patterns were associated with a better filtering ability. These epithelial and sub-epithelial microcystic areas have been hypothesized to be fluid-filled cysts, generated by the aqueous outflow throughout the bleb wall.

Lenzhofer and colleagues [24] confirmed that also after successful XGI, blebs with hypo-reflective cysts in the superficial layer were more likely to have a lower IOP.

In our study, we found a larger BECSA in trabeculectomy compared with XGI. These results are in line with those of Teus et al. [25] that reported a higher presence of hyporeflective cysts within the conjunctiva in trabeculectomy compared with XGI. Since BECSA positively correlated with BT,

Table 3 IVCM parameters of XEN gel implant and trabeculectomy groups

	MMD	MMA	SMR
XGI	198.49 ± 184.32	1709.41 ± 821.52	0.89 ± 0.67
Trabeculectomy	219.15 ± 212.45	2034.75 ± 793.87	1.53 ± 0.83
Mann-Whitney *U* test (*p* value)	0.524	0.021	0.011

XGI, XEN gel implantation; *MMD*, mean microcyst density (cysts/mm^2); *MMA*, mean microcyst area (mm^2); *SMR*, stromal meshwork reflectivity (arbitrary grading scale from grades 0 to 3)

this accounted for the thicker bleb wall in the trabeculectomy group. As microcysts are associated with the aqueous humor outflow, this result agrees with studies showing the correlation between the bleb-wall thickness and the filtering ability of the bleb [15, 17, 21, 31].

In accordance with previous findings, we found that blebs after XGI were flatter compared with trabeculectomy [25]. The relevance of the bleb height as an indicator of bleb function is still unclear and a matter of debate: in fact, while some studies did not find significant correlation between BH and bleb filtering ability [13, 15, 17], other studies reported significant correlation between BH and IOP [20, 21, 31].

The present study has some limitations. First, this was a retrospective study and we cannot state whether these differences are present also at different follow-up. Second, we included a relatively small sample of patients, with a medium-term follow-up; thus, prospective studies with a larger sample size and a longer follow-up are warranted to confirm our results. Third, we only included completely successful filtering blebs; therefore, further studies aimed at comparing failed blebs after XGI and trabeculectomy are warranted. Finally, further studies correlating IVCM and AS-OCT findings with classification systems could allow to verify whether the investigated parameters are in line with the clinical findings.

In conclusion, our study found that filtration blebs that develop after XGI and trabeculectomy are morphologically different, and differences can depend on the surgical technique and/or on the aqueous humor dynamics under the conjunctiva. XGI blebs appear flatter and thinner, with a higher number of epithelial cysts and a hypo-reflective bleb wall compared with trabeculectomy. These results should be taken into consideration since indicating that each type of filtration bleb presents specific morphological features according to the type of surgery; the knowledge of these aspects may help a clinician in the very early detection of filtration failure in each surgery.

Compliance with ethical standards

Conflict of interest The authors declare that they have no conflict of interest.

Ethical approval All procedures performed in studies involving human participants were in accordance with the ethical standards of the Ophthalmic Clinic, San Giuseppe Hospital, University of Milan, and the Ophthalmic Clinic, University G. d'Annunzio of Chieti-Pescara, Italy, and with the 1964 Helsinki Declaration and its later amendments or comparable ethical standards. This article does not contain any studies with animals performed by any of the authors.

Informed consent Informed consent was obtained from all individual participants included in the study.

References

1. European Glaucoma Society (2014) Terminology and guidelines for glaucoma, 4th edn. Editore Publi Comm, Savona, Italy, pp 1–191
2. Jampel HD, Musch DC, Gillespie BW, Lichter PR, Wright MM, Guire KE, Collaborative Initial Glaucoma Treatment Study Group (2005) Perioperative complications of trabeculectomy in the collaborative initial glaucoma treatment study (CIGTS). Am J Ophthalmol 140:16–22. https://doi.org/10.1016/j.ajo.2005.02.013
3. Lavia C, Dallorto L, Maule M, Ceccarelli M, Fea AM (2017) Minimally-invasive glaucoma surgeries (MIGS) for open angle glaucoma: a systematic review and meta-analysis. PLoS One 12: e0183142. https://doi.org/10.1371/journal.pone.0183142
4. Schlenker MB, Gulamhusein H, Conrad-Hengerer I et al (2017) Efficacy, safety, and risk factors for failure of standalone ab interno gelatin microstent implantation versus standalone trabeculectomy. Ophthalmology 124:1579–1588. https://doi.org/10.1016/j.ophtha.2017.05.004
5. Picht G, Grehn F (1998) Classification of filtering in trabeculectomy: biomicroscopy and functionality. Curr Opin Ophthalmol 9:2–8. https://doi.org/10.1097/00055735-199804000-00002
6. Kumaran A, Husain R, Htoon HM, Aung T (2018) Longitudinal changes in bleb height, vascularity, and conjunctival microcysts after trabeculectomy. J Glaucoma 27:578–584. https://doi.org/10.1097/IJG.0000000000000967
7. Cantor LB, Mantravadi A, WuDunn D, Swamynathan K, Cortes A (2003) Morphologic classification of filtering blebs after glaucoma filtration surgery: the Indiana Bleb Appearance Grading Scale. J Glaucoma 12:266–271. https://doi.org/10.1097/00061198-200306000-00015
8. Wells A, Ashraff N, Hall R, Purdie G (2006) Comparison of two clinical bleb grading systems. Ophthalmology 113:77–83. https://doi.org/10.1016/j.ophtha.2005.06.037
9. Labbé A, Dupas B, Hamard P, Baudouin C (2005) In vivo confocal microscopy study of blebs after filtering surgery. Ophthalmology 112:1979–1986. https://doi.org/10.1016/j.ophtha.2005.05.021
10. Messmer EM, Zapp DM, Mackert MJ, Thiel M, Kampik A (2006) In vivo confocal microscopy of filtering blebs after trabeculectomy. Arch Ophthalmol 124:1095–1103. https://doi.org/10.1001/archopht.124.8.1095
11. Guthoff R, Klink T, Schlunck G, Grehn F (2006) In vivo confocal microscopy of failing and functioning filtering blebs: results and clinical correlations. J Glaucoma 15:552–558. https://doi.org/10.1097/01.ijg.0000212295.39034.10
12. Amar N, Labbè A, Hmard P, Dupas B, Baudouin C (2008) Filtering blebs and aqueous pathway: an immunocytological and in vivo confocal microscopy study. Ophthalmology 115:1154–1161. https://doi.org/10.1016/j.ophtha.2007.10.024
13. Ciancaglini M, Carpineto P, Agnifili L, Nubile M, Lanzini M, Fasanella V, Mastropasqua L (2008) Filtering bleb functionality: a clinical, anterior segment optical coherence tomography and in vivo confocal microscopy study. J Glaucoma 17:308–317. https://doi.org/10.1097/IJG.0b013e31815c3a19
14. Ciancaglini M, Carpineto P, Agnifili L, Nubile M, Fasanella V, Mattei PA, Mastropasqua L (2009) Conjunctival characteristics in primary open-angle glaucoma and modifications induced by trabeculectomy with mitomycin C: an in vivo confocal microscopy study. Br J Ophthalmol 93:1204–1209. https://doi.org/10.1136/bjo.2008.152496
15. Singh M, Chew PT, Friedman DS et al (2007) Imaging of trabeculectomy blebs using anterior segment optical coherence tomography. Ophthalmology 114:47–53. https://doi.org/10.1016/j.ophtha.2006.05.078

16. Nakano N, Hangai M, Nakanishi H, Inoue R, Unoki N, Hirose F, Ojima T, Yoshimura N (2010) Early trabeculectomy bleb walls on anterior-segment optical coherence tomography. Graefes Arch Clin Exp Ophthalmol 248:1173–1182. https://doi.org/10.1007/s00417-010-1311-3
17. Tominaga A, Miki A, Yamazaki Y, Matsushita K, Otori Y (2010) The assessment of the filtering bleb function with anterior segment optical coherence tomography. J Glaucoma 19:551–555. https://doi.org/10.1097/IJG.0b013e3181ca76f3
18. Hirooka K, Takagishi M, Baba T, Takenaka H, Shiraga F (2010) Stratus optical coherence tomography study of filtering blebs after primary trabeculectomy with a fornix-based conjunctival flap. Acta Ophthalmol 88:60–64. https://doi.org/10.1111/j.1755-3768.2008.01401.x
19. Pfenninger L, Schneider F, Funk J (2011) Internal reflectivity of filtering blebs versus intraocular pressure in patients with recent trabeculectomy. Invest Ophthalmol Vis Sci 52:2450–2455. https://doi.org/10.1167/iovs.10-5520
20. Kokubun T, Tsuda S, Kunikata H, Himori N, Yokoyama Y, Kunimatsu-Sanuki S, Nakazawa T (2018) Anterior-segment optical coherence tomography for predicting postoperative outcomes after trabeculectomy. Curr Eye Res 43: 762–770. https://doi.org/10.1080/02713683.2018.1446535
21. Waibel S, Spoerl E, Furashova O, Pillunat LE, Pillunat KR (2019) Bleb morphology after mitomycin-C augmented trabeculectomy: comparison between clinical evaluation and anterior segment optical coherence tomography. J Glaucoma 28:447–451. https://doi.org/10.1097/IJG.0000000000001206
22. Olate-Pérez Á, Pérez-Torregrosa VT, Gargallo-Benedicto A, Neira-Ibáñez P, Cerdà-Ibáñez M, Osorio-Alayo V, Barreiro-Rego A, Duch-Samper A (2017) Prospective study of filtering blebs after XEN45 surgery. Arch Soc Esp Opthalmol 92:366–371. https://doi.org/10.1016/j.oftal.2017.02.010
23. Fea AM, Spinetta R, Cannizzo PML, Consolandi G, Lavia C, Aragno V, Germinetti F, Rolle T (2017) Evaluation of bleb morphology and reduction in IOP and glaucoma medication following implantation of a novel gel stent. J Ophthalmol 2017:9364910. https://doi.org/10.1155/2017/9364910
24. Lenzhofer M, Strohmaier C, Hohensinn M et al (2019) Longitudinal bleb morphology in anterior segment OCT after minimally invasive transscleral ab interno Glaucoma Gel Microstent implantation. Acta Ophthalmol 97:e231–e237. https://doi.org/10.1111/aos.13902
25. Teus MA, Paz Moreno-Arrones J, Castaño B, Castejon MA, Bolivar G (2019) Optical coherence tomography analysis of filtering blebs after long-term, functioning trabeculectomy and XEN® stent implant. Graefes Arch Clin Exp Ophthalmol 257:1005–1011. https://doi.org/10.1007/s00417-019-04272-8
26. Mastropasqua L, Agnifili L, Mastropasqua R, Fasanella V, Nubile M, Toto L, Carpineto P, Ciancaglini M (2014) In vivo laser scanning confocal microscopy of the ocular surface in glaucoma. Microsc Microanal 20:879–994. https://doi.org/10.1017/S1431927614000324
27. Mastropasqua R, Fasanella V, Brescia L, Oddone F, Mariotti C, Di Staso S, Agnifili L (2017) In vivo confocal imaging of the conjunctiva as a predictive tool for the glaucoma filtration surgery outcome. Invest Opthalmol Vis Sci 58:BIO114–BIO120. https://doi.org/10.1167/iovs.17-21795
28. Agnifili L, Fasanella V, Mastropasqua R, Frezzotti P, Curcio C, Brescia L, Marchini G (2016) In vivo goblet cell density as a potential indicator of glaucoma filtration surgery outcome. Invest Ophthalmol Vis Sci 57:2928–2935. https://doi.org/10.1167/iovs.16-19257
29. Fluorouracil Filtering Surgery Study Group Fluorouracil Filtering Surgery Study one-year follow-up. Am J Ophthalmol 186:33–42. https://doi.org/10.1016/j.ajo.2017.12.021
30. Huang D, Swanson EA, Lin CP et al (1991) Optical coherence tomography. Science 254:1178–1181. https://doi.org/10.1126/science.1957169
31. Narita A, Morizane Y, Miyake T, Seguchi J, Baba T, Shiraga F (2018) Characteristics of early filtering blebs that predict successful trabeculectomy identified via three-dimensional anterior segment optical coherence tomography. Br J Ophthalmol 102:796–801. https://doi.org/10.1136/bjophthalmol-2017-310707